

## Nck $\beta$ Interacts with Tyrosine-Phosphorylated Disabled 1 and Redistributes in Reelin-Stimulated Neurons

Albena Pramatarova, Pawel G. Ochalski, Kelian Chen, Andrea Gropman, Sage Myers, Kyung-Tai Min, and Brian W. Howell\*

Neurogenetics Branch, National Institute of Neurological Disorders and Stroke, National Institutes of Health, Bethesda, Maryland 20892-1250

Received 23 January 2003/Returned for modification 12 March 2003/Accepted 10 July 2003

**The tyrosine phosphorylation sites of the Disabled 1 (Dab1) docking protein are essential for the transmission of the Reelin signal, which regulates neuronal placement. Here we identify Nck $\beta$  as a phosphorylation-dependent, Dab1-interacting protein. The SH2 domain of Nck $\beta$  but not Nck $\alpha$  binds Dab1 phosphorylated on the Reelin-regulated site, Y220, or on Y232. Nck $\beta$  is coexpressed with Dab1 in the developing brain and in cultured neurons, where Reelin stimulation leads to the redistribution of Nck $\beta$  from the cell soma into neuronal processes. We found that tyrosine-phosphorylated Dab1 in synergy with Nck $\beta$  disrupts the actin cytoskeleton in transfected cells. In *Drosophila melanogaster*, exogenous expression of mouse Dab1 causes tyrosine phosphorylation site-dependent morphological changes in the compound eye. This phenotype is enhanced by overexpression of the *Drosophila* Nck protein Dock, suggesting a conserved interaction between the Disabled and Nck family members. We suggest a model in which Dab1 phosphorylation leads to the recruitment of Nck $\beta$  to the membrane, where it acts to remodel the actin cytoskeleton.**

The *Dab1* gene, which encodes a cytoplasmic docking protein, plays an essential, cell-autonomous role during brain development (15, 17, 26, 44, 51). Animals that lack a functional *Dab1* gene have anomalies in the formation of neuronal laminae in the cerebral cortex, hippocampus, and cerebellum, as well as defects in the olfactory bulbs and spinal cord (26, 44, 45, 51, 52). In mammals, neuronal placement is regulated by a number of genes encoding transcription factors, extracellular matrix proteins, receptor molecules, kinases, and actin and tubulin binding proteins (16, 19, 36, 40, 42). Among these, three have been shown to affect Dab1 function through a linear signaling pathway, the *Reelin* gene and two genes encoding members of the low-density lipoprotein (LDL) receptor family, VLDLR and ApoER2 (19, 40).

The protein encoded by the *Reelin* gene, a secreted glycoprotein produced in discrete regions of the developing brain (10, 38), physically interacts with the extracellular domains of the VLDLR and ApoER2 transmembrane proteins expressed on migrating neurons (2, 9, 20). These partially redundant receptors bind to an N-terminal domain in Dab1, the PTB domain, through an N-P-X-Y peptide sequence in their cytoplasmic domains (29, 46, 47). The formation of the Reelin-receptor interaction is a requisite for Reelin-induced Dab1 tyrosine phosphorylation. This was shown by blocking the binding of Reelin to the receptors biochemically and, more recently, by Reelin stimulation experiments with neurons cultured from mice that lacked both receptors, where Dab1 phosphorylation did not occur (2, 9, 20). During brain development, the level of Dab1 tyrosine phosphorylation is lower in Reelin mutants than in wild-type animals (27). Taken together, these data point to Dab1 tyrosine phosphorylation as an out-

come of Reelin action on neurons during the formation of the nervous system.

Five residues proximal to the Dab1 PTB domain account for all of the tyrosine phosphorylation sites utilized during brain development (28). Reelin induces phosphorylation of two of these, Y198 and Y220, in vitro (32). A third tyrosine, Y232, is not detectably phosphorylated in cultured neurons but is phosphorylated in embryonic brain (B. Howell, unpublished results) and is phosphorylated in transfected cells in the presence of the Src kinase (32). The phosphorylation sites are required to rescue the Dab1 null phenotype (28). An expression cassette that contains either a wild-type or mutant cDNA for Dab1 restores expression of the Dab1 protein when integrated into the *dab1* gene locus. However, only the wild-type Dab1, not the tyrosine phosphorylation site-substituted Dab1 (Dab1-5F), is capable of restoring normal brain development. Understanding the role of the Dab1 phosphorylation sites is therefore central to the resolution of the downstream consequences of Reelin action.

The SH2 domain-containing proteins Src, Fyn, and Abl have previously been shown to bind Dab1 in a phosphotyrosine-dependent manner in vitro (25). Recently, it was revealed that the Src family kinases, including Src, Fyn, and Yes, are the predominant kinases required for the high stoichiometry of Dab1 phosphorylation observed during development and Reelin stimulation (1, 3). The activity of the Src, Fyn, and Yes kinases is increased by Reelin treatment of primary neurons in a manner that requires Dab1 for full activation (1, 3), and they therefore likely act upstream and downstream of Dab1 tyrosine phosphorylation.

Here we identify a novel phosphotyrosine-dependent Dab1-binding partner, the SH2-SH3 adaptor molecule Nck $\beta$ . The Dab1-Nck $\beta$  interaction required the Nck $\beta$  SH2 domain and Dab1 tyrosine phosphorylation sites. Reelin stimulation resulted in the redistribution of Nck $\beta$  into the processes of cul-

\* Corresponding author. Mailing address: Neurogenetics Branch, NINDS/NIH, 10 Center Dr., Bethesda, MD 20892-1250. Phone: (301) 435-1835. Fax: (301) 480-3365. E-mail: howellb@ninds.nih.gov.

tured neurons. In addition, we show that overexpression of Nck $\beta$  in cultured fibroblasts alters the actin cytoskeleton when coexpressed with tyrosine-phosphorylated Dab1. In *Drosophila melanogaster*, the conserved Nck family member Dock is thought to regulate cytoskeletal dynamics required for axon guidance and target recognition (13, 14). We show that overexpression of the *Drosophila* Nck protein Dock enhances phenotypes caused by exogenous expression of mouse Dab1 in the *Drosophila* eye. This enhancement is dependent upon the Dab1 tyrosine phosphorylation sites. We propose that during mouse development, tyrosine-phosphorylated Dab1 recruits Nck $\beta$  to membrane compartments where this complex acts to remodel the actin cytoskeleton.

#### MATERIALS AND METHODS

**Plasmids.** The vector pBTM116-Dab PTB-5Y(Src) was constructed by ligating the *SalI*-cut parental vector pBTM116(Src) (gift from M. Liubin) (35) with the *XhoI*-digested PCR product from the mouse *Dab1* cDNA and primer pair BTM5 (GCGCTCGAGGGATGCTCAACTGAGACAGA) and BTM5Y (GCGCTC GAGCTAATCAGGAGGGGTGGACATGTCTCC). This construct encodes the LexA DNA binding domain fused to residues 1 to 257 of Dab1, which includes the PTB domain and the tyrosine phosphorylation sites.

The GSTDab1-276 fusion proteins were constructed to express residues 1 to 276 of Dab1 by ligating *Bam*HI- and *Eco*RI-digested PCR products of the primer pair DabBamATG (CGCGGATCCAGGATGCTCAACTGAG) and DabStop276 (GCGGAATTCCTAGGACGACGACGGGAG) into the respective sites in pGex-2T (Pharmacia). The generation of the tyrosine to phenylalanine substitutions in Dab1 has been described elsewhere (28). The pDsDab1RFP and pDsDab1RFP-5F clones were generated by subcloning the mouse *Dab1* cDNA from the clone pBSDab555 (25) or the Dab1-5F mutant, respectively (28), into the pDsRed2 vector (Clontech) between the *XhoI* and *Bam*HI sites to produce a full-length fusion protein with the red fluorescent protein (RFP) C-terminal to Dab1 residues 1 to 555. The restriction sites were introduced by PCR with primers GGCCTCGAGGCCACCATGCTCAACTGAGACAGAAGCTTC and CGCGGATCCGCGCTACCGTCTGTGGACTTAT.

The pDsDab1-wt clone was created by inserting a stop codon, after residue 555, of Dab1 by swapping the *XmnI*-*Bam*HI fragment from pBSDab555 into the pDSdab1RFP vector. The pRK5-based hemagglutinin (HA)-Nck $\alpha$  and HA-Nck $\beta$  expression vectors and the generation of the mutants Nck $\beta$ -R312K and Nck $\beta$ -W39,149,235K have been described elsewhere, and these vectors were the kind gift of Wei Li (7). To generate the pINDY6-UAS vectors used to generate the transgenic flies, we restricted the pDSRed vectors with *NorI*, blunted this site with T4 DNA polymerase, and then cut with *XhoI* to excise the RFP, Dab1RFP, and Dab1RFP-5F coding regions. These cDNA fragments were then ligated into the *XhoI* and *StuI* sites in pINDY6, which placed the coding regions downstream of 5' UAS sequences to generate the UAS-RFP, UAS-Dab1RFP, and UAS-Dab1RFP-5F constructs.

**Yeast two-hybrid screen.** The protocol for the two-hybrid screen was described in detail previously (50). Briefly, we transformed the L40 strain of *Saccharomyces cerevisiae*, which has *lexA* operator sequences 5' to the *HIS3* and *lacZ* reporter genes, with the pBTM116 Dab1 PTB-5Y(Src) plasmid. Colonies that grew up on tryptophan-free medium, suggesting the presence of pBTM116-derived plasmid, were tested for the expression of Src by Western blotting yeast cell lysates with the antiphosphotyrosine antibody 4G10 (Upstate Biotechnology). A single positive transfectant was expanded and transformed with a neonatal mouse brain library (29) in the Clontech pGADGH vector, which expresses proteins as fusions with the GAL4 activation domain.

A nonsaturating screen of 100,000 transformants yielded 50 clones that grew up on the selective medium lacking histidine, suggesting a potential protein-protein interaction between the LexA-Dab1 fusion protein and the GAL4 mouse brain fusion. These 50 transformants were isolated and retested for  $\beta$ -galactosidase expression by filter assay (50). Only 3 of the 50 original had  $\beta$ -galactosidase signals that were above the vector-alone background control. The pGADGH library plasmids were rescued from the *S. cerevisiae* cells by standard methods and sequenced with an ABI Prism sequencer with both the Gad GH 5' oligonucleotide (CTATTCGATGGTGAAGATACC) and the M13 forward primer (Stratagene).

**In vitro association and coimmunoprecipitation experiments.** HEK293T cells ( $5 \times 10^6$ ) were transfected with the pRK5HA-Nck vectors (3  $\mu$ g) alone by

incubating with Fugene (in a ratio of 1:3; Roche) in serum-free medium for 15 min before addition to cells. Two days later, transfected cells were lysed on ice in 1 ml of TX-IPB (0.1 M NaCl, 1% Triton X-100, 10 mM HEPES [pH 7.4], 2 mM EDTA, 50 mM NaF, 1 mM phenylarsine oxide, 0.1% 2-mercaptoethanol, protease cocktail [complete mini, EDTA free; Roche]). After a 10-min incubation on ice, the lysates were clarified by centrifugation at  $20,000 \times g$  for 20 min. Clarified lysates were incubated with the indicated glutathione *S*-transferase (GST)-Dab1-276 fusion proteins (3  $\mu$ g.) immobilized on glutathione Sepharose (Pharmacia) for 2 h at 4°C, and washed four times with TX-IPB.

Bound proteins were eluted with 100 mM phenylphosphate buffer (6), mixed with an equal volume of 2 $\times$  sample buffer (4% sodium dodecyl sulfate, 40% glycerol, 0.2 M Tris-HCl [pH 6.8], 5.6 M 2-mercaptoethanol, 5 mM EDTA, 0.02% bromophenol blue) and boiled for 5 min prior to analysis by sodium dodecyl sulfate-polyacrylamide gel electrophoresis (PAGE) and Western blotting with antihemagglutinin antigen polyclonal antibody (Santa Cruz). The same binding pattern was observed when sample buffer was used for the elutions. Tyrosine phosphorylation of the GST-Dab1-276 fusions was done with Abl kinase (100 U; New England Biologicals) at 30°C for 30 min in 1 $\times$  kinase buffer (50 mM Tris-HCl [pH 7.5], 10 mM MgCl<sub>2</sub>, 1 mM EGTA, 2 mM dithiothreitol, 0.01% Brij 35, 10 mM ATP). The native GST protein was not tyrosine phosphorylated by Abl kinase. With phosphorylation-specific antibodies, we were able to show specific phosphorylation of tyrosines 198, 220, and 232 of Dab1 (data not shown).

For coimmunoprecipitation experiments, HEK293T cells were transfected with DNAs in the ratio of pDSDab1 (5  $\mu$ g), pRK5HA-Nck $\beta$  (1  $\mu$ g), and pLXSH SrcY527F (1  $\mu$ g) (28). For control samples, substitutions with pcDNA3.1 (Invitrogen) were made in equal amounts to hold the total amount of DNA in transfections constant. Cell lysis and clarification were done as described above, but additional clarification was accomplished by mixing the lysates with protein A-Sepharose beads for 15 min before finally collecting the supernatant for immunoprecipitation analysis. Clarified cell lysates were incubated with anti-Dab1 polyclonal antibody (2  $\mu$ l; Chemicon) or with anti-HA antibody (5  $\mu$ l; Santa Cruz) that had previously been bound and chemically cross-linked to protein A-Sepharose with dimethyl pimelimidate (43). Proteins were eluted in 1 $\times$  sample buffer, boiled for 10 min, and resolved by 7.5% PAGE prior to Western blotting with various antibodies.

**Reelin stimulations of primary neuronal cultures.** Reelin- and control-conditioned media were prepared as previously described with some modifications (27). HEK293T cells were transfected with the Reelin-encoding vector pCrl or with a mock pcDNA3 vector (12). After 24 h the cells were transferred to bacterial dishes in Opti-MEM serum-free media (Invitrogen). Reelin-conditioned media and the control-conditioned media were collected at 48, 72, and 96 h posttransfection, concentrated 10-fold with a Centricon centrifugal filter with a 100,000-molecular-weight cutoff (Millipore), and stored at  $-80^\circ\text{C}$  in small aliquots.

Primary neuronal cultures were established by using forebrains from embryonic day 16.5 (E16.5) embryos from a Reelin heterozygous cross. Each embryo was processed individually, and tissue samples were taken for Reelin genotyping according to the published protocol (11). The forebrains were dissected in ice-cold Ca<sup>2+</sup>- and Mg<sup>2+</sup>-free Hanks balanced salt solution (HBSS; Invitrogen) and incubated in 0.25% trypsin-1 mM EDTA for 15 min at 37°C. The tissue was washed three times with HBSS and dissociated with a fire-polished glass Pasteur pipette in HBSS containing 0.025% DNase I, 0.4 mg of soy bean trypsin inhibitor/ml, 3 mg of bovine serum albumin/ml, and 12 mM MgSO<sub>4</sub>. The dissociated cells were then washed three times in HBSS and resuspended in Neurobasal medium (Invitrogen) supplemented with 4% B-27 and 2.92 mg of glutamine, 100 U of penicillin, and 100 mg of streptomycin (Invitrogen)/ml. Neurons from each animal were plated on 12 poly-L-lysine- and entactin-collagen IV-laminin (Upstate Biotechnology)-coated 18-mm glass coverslips and grown in a 12-well dish for 24 h at 37°C prior to Reelin stimulation.

Neurons homozygous for mutant Reelin were used in all the studies on primary neurons presented in this paper and consistently gave more-dramatic results than heterozygous or wild-type neurons. Stimulations were done by replacing the growth media with Reelin-conditioned or control-conditioned media and incubating the cells at 37°C for 10 to 30 min prior to fixation and processing for immunocytochemistry.

All mice used to generate tissues used in this paper were handled under the animal care and use guidelines of the National Institutes of Health.

**Immunocytochemistry.** Rat-2 fibroblasts were plated in 60-mm dishes and transiently transfected with 2  $\mu$ g of each DNA with Fugene (Invitrogen) as described above. The average expression of Nck $\beta$  in transfected cells was three- to fivefold higher than endogenous levels as determined by immunocytochemistry with an anti-Nck $\beta$  antibody (Upstate Biotechnology). DNA combinations in

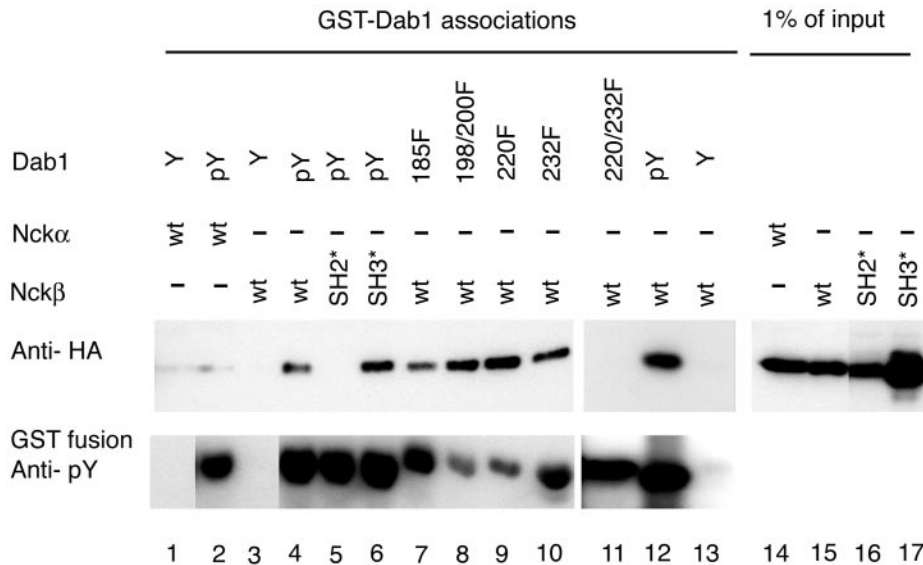


FIG. 1. Dab1 tyrosine phosphorylation and the Nck $\beta$  SH2 domain are required for complex formation. Nck proteins were detected by anti-HA Western blotting (upper panel) of cell lysates from HEK293T cells transfected with Nck $\alpha$  (lanes 1, 2, and 14), Nck $\beta$  (lanes 3, 4, 7 to 13, and 15), Nck $\beta$ -R312K carrying a mutation in the SH2 domain (lanes 5 and 16), or Nck $\beta$ -W39,149,235K, which has mutations in all three SH3 domains (lanes 6 and 17). The proteins that bound the various GST-Dab1 fusion proteins were eluted by phenyl phosphate-containing buffer (lanes 4 to 17; upper panel). The GST-Dab1 fusions included Dab1-wt (lanes 1 to 6, 12, and 13), Dab1-Y185F (lane 7), Dab1-Y198,200F (lane 8), Dab1 Y220F (lane 9), Dab1 Y232F (lane 10), and Dab1 Y220,232F (lane 11) in their unphosphorylated state (Y; lanes 1, 3, and 13) or after tyrosine phosphorylation by Abl (pY or mutant designation, lanes 2 and 4 to 12). All GST fusion proteins incubated with Abl kinase were tyrosine phosphorylated as determined by Western blotting with antiphosphotyrosine antibody 4G10 (lower panel). Lanes 14 to 17 represent 1% of the amount of cell lysate used in the association assay (lanes 1 to 13).

the order presented in Fig. 8 are as follows: pRK5HA-Nck $\beta$  and pcDNA3, pDsDab1RFP and pcDNA3, pDsDab1RFP and pRK5HA-Nck $\beta$ , pDsDab1-wt and pRK5HA-Nck $\beta$ , pDsDab1RFP-5F and pRK5HA-Nck $\beta$ , and pDsDab1RFP and pRK5HA-Nck $\beta$ -R312K SH2 domain mutant. After 24 h, the cells were plated on poly-L-lysine-coated glass coverslips and grown for an additional 24 h prior to fixation.

The cells on coverslips were washed once with phosphate-buffered saline (PBS), fixed in 4% paraformaldehyde in PHEM buffer (60 mM PIPES [pH 7.0], 25 mM HEPES [pH 7.0], 10 mM EGTA [pH 8.0], 2 mM MgCl<sub>2</sub>, 0.12 M sucrose) for 20 min at room temperature for immunostaining or for 30 min at 37°C for actin staining, followed by permeabilization with 0.1% saponin for 10 min. All immunofluorescence detection was performed in 3% bovine serum albumin–2% normal donkey serum in PBS. The Reelin-treated neurons were probed sequentially with a rabbit anti-Nck $\beta$  antibody at 1:100 dilution (Upstate), a fluorescein isothiocyanate (FITC)-conjugated donkey anti-rabbit antibody (Jackson ImmunoResearch Laboratories), and finally a rabbit anti-Dab1-B3-Cy3 antibody diluted 1:100 (25). The Rat-2 cells were probed with a mouse anti-HA antibody diluted 1:50 (Santa Cruz Biotechnology) and, for the cells transfected with the pDsDab1-wt clone, with the rabbit anti-Dab1-B3 antibody diluted 1:100, followed by a donkey anti-mouse antibody (conjugated to Cy5 for actin staining or to FITC for colocalization) and a Texas Red-conjugated donkey anti-rabbit antibody (Jackson ImmunoResearch Laboratories). The actin cytoskeleton was stained with Alexa Fluor 594 phalloidin (red) for the neurons and with Bodipy FL phalloidin (green) in the rest of the transfection experiments. The coverslips were finally incubated with DAPI (4',6'-diamidino-2-phenylindole) to detect cell nuclei and mounted in Vectashield (Vector Laboratories).

Mouse brains were dissected from animals perfused with ice-cold PBS followed by 4% paraformaldehyde, infiltrated with 30% sucrose, and frozen in Tissue-Tek OCT compound (Sakura Finetechnical Co.). Immunostaining was performed using the rabbit anti-Nck $\beta$  antibody diluted 1:300 (Upstate Biotechnology), followed by a FITC-conjugated donkey anti-rabbit antibody (Jackson ImmunoResearch Laboratories), and finally the rabbit anti-Dab1-B3-indocarbocyanine antibody diluted 1:100 (25). The sections were then stained with DAPI and mounted in Vectashield (Vector Laboratories). Images were acquired digitally with a DeltaVision microscope (Applied Precision) and deconvolved with the softWoRx algorithm (Applied Precision) to remove out-of-focus light from the image.

**Drosophila stocks and culture.** All fly culture genetics and production of the transgenics were done according to standard protocols. The w<sup>1118</sup> strain was used to generate the transgenic lines. Multiple independent transformant lines were established and analyzed by Western blotting and fluorescence microscopy to assay protein expression. The *UAS-Dock* transgenic flies were a gift from L. Zipursky. Lines homozygous for *UAS-RFP*, *UAS-Dab1RFP*, *UAS-Dab1RFP-5F*, *UAS-Dock*, *UAS-Dock*; *UAS-Dab1RFP*, and *UAS-Dock*; *UAS-Dab1RFP-5F* were generated and crossed with flies homozygous for *GMR-GAL4* to generate the flies shown in Fig. 10.

**Scanning electron microscopy.** Adult flies were fixed in 2.5% glutaraldehyde in 0.1 M cacodylate buffer overnight at 4°C. Flies were washed with 0.1 M cacodylate buffer and dehydrated through a graded series of ethanol washes. Next, flies were incubated in hexamethyldisilazane (HMDS; Electron Microscopy Sciences [EMS]) twice. Samples were air dried under low vacuum, mounted with silver conduction paint (EMS), sputter coated with Pd-Au wire in a Denton vacuum evaporator, and visualized with a Hitachi S570 scanning electron microscope.

## RESULTS

**Identification of Nck $\beta$  as a Dab1 binding protein.** Since the Dab1 tyrosine phosphorylation sites are critical for Dab1 function, we sought to identify binding partners of Dab1 dependent on these sites. We did this with a modified yeast two-hybrid screen, in which expression of the tyrosine kinase Src ensured Dab1 tyrosine phosphorylation (31). This screen was predicted to identify proteins that interact with Dab1 in both a phosphotyrosine-dependent and -independent manner.

The PTB domain and downstream tyrosine phosphorylation sites were fused with the LexA DNA binding site and used to screen a library of neonatal mouse brain cDNAs expressed as fusions with the Gal4 transactivator. Three interacting proteins were identified. Two of these were members of the amyloid precursor protein (APP) family and have been identified from

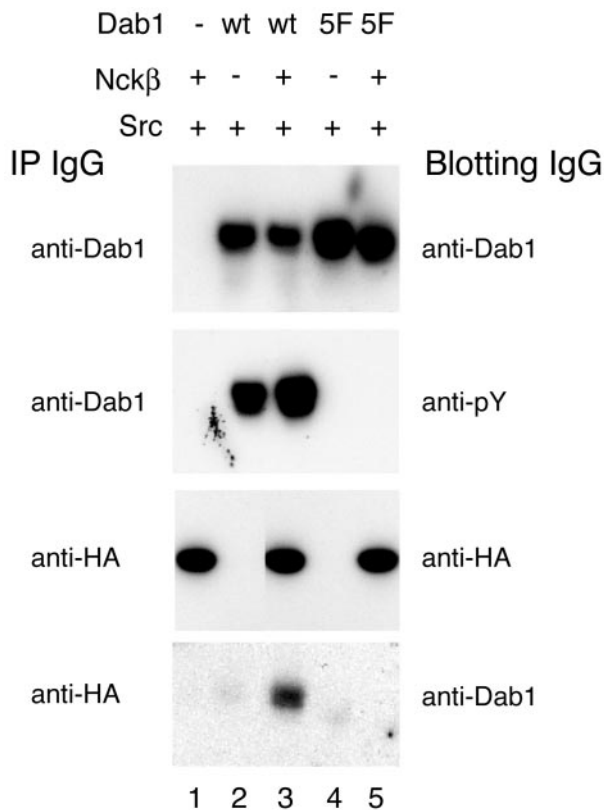


FIG. 2. Nckβ coimmunoprecipitates with tyrosine-phosphorylated Dab1 but not the unphosphorylated Dab1-5F mutant. Immunoprecipitations with anti-Dab1 or anti-HA antibody, as indicated to the left of the panels, were done from lysates of HEK293T cells transfected with SrcY527F (lanes 1 to 5) and combinations of Nckβ (lanes 1, 3, and 5) and Dab1 wild-type (lanes 2 and 3) or Dab1-5F (lanes 4 and 5). Immunoprecipitation of Dab1 with an anti-C-terminal antibody followed by Western blotting with anti-Dab1 (B3) (top panel) shows that transfected cells express at least as much mutant Dab1-5F as wild-type Dab1, but immunoblotting with antiphosphotyrosine antibody (4G10; second panel) shows that only the wild-type Dab1 was tyrosine phosphorylated. Equal amounts of Nckβ were immunoprecipitated from all HA-Nckβ-transfected cells (third panel, lanes 1, 3, and 5), yet Dab1 was only detected in anti-HA immunocomplexes (bottom panel) from cells expressing both Nckβ and wild-type Dab1 (lane 3).

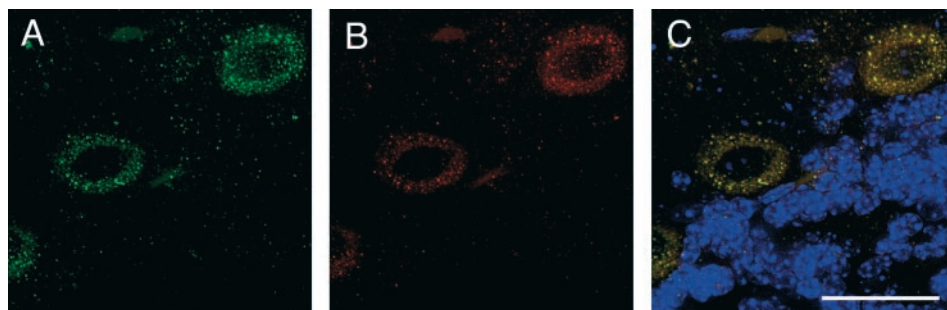


FIG. 3. Nckβ is expressed in Dab1-expressing Reelin-responsive cells. (A) The Nckβ protein is detected in the cell bodies of Purkinje cells, which also express Dab1 (B) in the brains of adult mice. (C) Both Dab1 and Nckβ are absent from the internal granule cell layer, which is apparent below the Purkinje cells with the nuclear indicator DAPI. Bar, 10 μm.

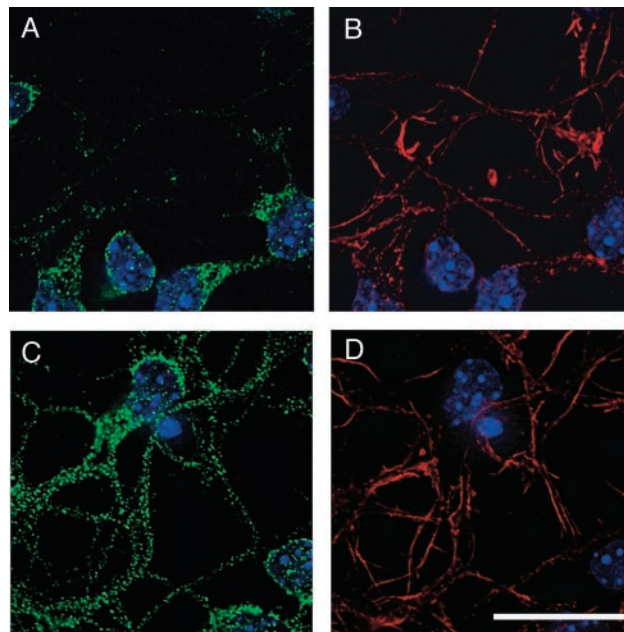


FIG. 4. Nckβ is redistributed into neuronal processes after Reelin stimulation. (A and B) In cultures treated with control conditioned medium for 30 min, Nckβ (A; green) is found predominantly in the cell soma. (C and D) After Reelin treatment, Nckβ (C; green) is apparent in the majority of processes. Processes were detected (B and D) with fluorescently labeled phalloidin to visualize filamentous actin (red), and nuclei were detected with DAPI. Bar, 20 μm.

other Dab1 interaction screens (23, 29, 46). The cytoplasmic domains of APP and APLP1 have been shown to interact with the isolated Dab1 PTB domain in the absence of tyrosine phosphorylation (23, 29, 46). The third clone, Nckβ, has not previously been shown to interact with Dab1. This Nckβ isolate contains residues 201 through the termination codon, including the third SH3 domain as well as the sole SH2 domain.

**Association of Nckβ but not Nckα with tyrosine-phosphorylated Dab1.** Since the Nckβ clone isolated in the yeast two-hybrid screen contained the C-terminal-most SH3 domain and the SH2 domain, either or both domains could have mediated the interaction with Dab1. To validate the association and test which domain is required for the interaction between Nckβ and Dab1, we established an *in vitro* binding assay. A GST

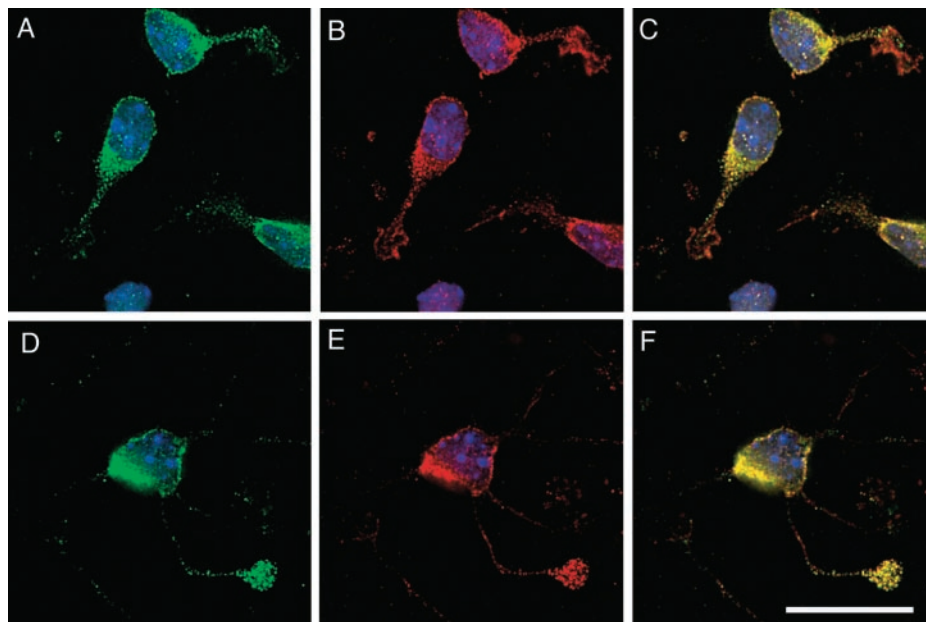


FIG. 5. Nck $\beta$  colocalizes with Dab1 in process termini after Reelin stimulation. (A to C) Nck $\beta$  (green; A and C) is predominantly found in the soma of primary neurons from Reelin mutant animals fixed after 10-min treatments with control conditioned medium, while Dab1 (red; B and C) was found throughout the neuron. Colocalization between Nck $\beta$  and Dab1 was observed in the cell soma but not in the processes (yellow; C). (D to F) After treatment with Reelin-conditioned medium for 10 min prior to fixation, Nck $\beta$  (D and F) was detected in processes with Dab1 (E and F), and colocalization (F) was apparent near the process termini. Bar, 20  $\mu$ m.

fusion with Dab1 that expresses the same region used in the two-hybrid screen, residues 1 to 257 of Dab1, was used either unphosphorylated or after tyrosine phosphorylation by Abl kinase to test the binding of Nck $\beta$  from lysates of transfected HEK293T cells. The same strategy was used to test binding of the closely related adaptor molecule Nck $\alpha$ . The GST-Dab1 fusion protein was immobilized on Sepharose and incubated with lysates from HEK293T cells transfected with HA-tagged versions of either Nck $\alpha$ , Nck $\beta$ , Nck $\beta$ -R312K, that has a defective SH2 domain, or Nck $\beta$ -W39,149,235K, which has three defective SH3 domains (Fig. 1).

Nck $\beta$  bound to the tyrosine-phosphorylated Dab1 fusion but not the unphosphorylated fusion. Interestingly, Nck $\alpha$  did not bind to the Dab1 fusion protein regardless of its phosphorylation. We sequenced the HA-Nck $\alpha$ -expressing vector to ensure that the SH2 domain was intact and found it to be free of errors. Mutation of the SH2 domain of Nck $\beta$  prevented binding, but mutation of all three SH3 domains of Nck $\beta$  had little or no effect on the interaction with tyrosine-phosphorylated Dab1. Nck $\beta$  bound well to tyrosine-phosphorylated GST-Dab1 fusions with substitutions of tyrosines to phenylalanine at positions 185, 198 and 200, 220, or 232, suggesting that the interaction was not mediated by a single phosphorylation site on Dab1. We found, however, that the Dab1 Y220,232F double mutant did not support binding to Nck $\beta$ . All GST-Dab1 fusions, including the Y220,232F mutant, were tyrosine phosphorylated by Abl kinase (Fig. 1). This shows that phosphorylation of either Y220 or Y232 was sufficient for the interaction.

To determine if the affinity of the Dab1 and Nck $\beta$  interaction was high enough to support binding *in vivo*, we assayed for coimmunoprecipitation of Dab1 and Nck $\beta$  from transfected

cells. This assay would also help determine if the C-terminal sequences absent from both the yeast two-hybrid screen and the *in vitro* binding assay might support binding to Dab1 in a phosphotyrosine-independent manner. To maximize Dab1 tyrosine phosphorylation, we expressed Dab1 in HEK293T cells in the presence of the activated Src mutant SrcY527F. Dab1 expression and tyrosine phosphorylation were examined by immunoprecipitating Dab1 and Western blotting with anti-Dab1 and anti-phosphotyrosine antibodies. Equal levels of Dab1 were observed in the Dab1 immunoprecipitates from cells transfected with cDNAs for Dab1-wt or Dab1-5F, but only Dab1-wt was tyrosine phosphorylated (Fig. 2), consistent with previous studies (28, 32).

Equal amounts of HA-tagged Nck $\beta$  (HA-Nck $\beta$ ) were recovered from all HA-Nck $\beta$ -transfected cells by immunoprecipitation with the anti-HA antibody (Fig. 2). Dab1, however, was only detected in the anti-HA immunoprecipitate from cell lysates having both wild-type, tyrosine-phosphorylated Dab1 and Nck $\beta$ . The unphosphorylated Dab1-5F protein was not detected in anti-HA immunoprecipitates, suggesting that Dab1 tyrosine phosphorylation sites are required for the interaction. Dab1 was not detected in immunocomplexes from cells not expressing HA-Nck $\beta$ , suggesting that Dab1 does not precipitate nonspecifically under the assay conditions. We were unable to detect HA-Nck $\beta$  in the Dab1 immunoprecipitates. This may suggest that only a small fraction of HA-Nck $\beta$  interacts with Dab1 under these conditions.

Other phosphoproteins may compete with Dab1 for binding to the Nck $\beta$  SH2 domain. The requirement of the tyrosine phosphorylation sites for the coimmunoprecipitation supports the evidence from the *in vitro* study that the SH2 domain, and not the SH3 domains, of Nck $\beta$  is sufficient for binding to Dab1.

In addition, the SH3 domains of Nck $\beta$  did not support a high-affinity interaction with C-terminal residues of Dab1 absent from the yeast two-hybrid screen or the GST-Dab1 binding assay.

**Nck $\beta$  is expressed in embryonic neurons.** As a minimum requirement for Nck $\beta$  to collaborate with Dab1 in Reelin signal transduction, it must be expressed in Reelin-responsive cells in the developing brain. We therefore examined Nck $\beta$  protein levels in mouse brain by Western blot at E16.5, a time when Dab1 phosphorylation levels have been shown to be Reelin dependent (27). A single band corresponding to Nck $\beta$  was detected in total brain lysates of animals wild-type, heterozygous, or homozygous for mutations in the *Reelin* gene (data not shown). The protein level did not vary between samples, suggesting that Nck $\beta$  protein levels are not down-regulated by Reelin signaling, unlike Dab1 (41). The Nck $\beta$  antibody (Upstate) was raised to peptide sequences not found in Nck $\alpha$ , and it did not recognize anti-HA immunoreactive HA-Nck $\alpha$  in Western blots (data not shown). This demonstrates that Nck $\beta$  is expressed in the embryonic brain at times when the Reelin signaling pathway is regulating neuronal positioning and that the antibody is specific.

We detected Dab1 expressed broadly in the cerebral cortex of embryonic animals at E15.5 (data not shown), suggesting that it is expressed in the correct cell populations to play a role in Reelin signaling. In addition, we detect Nck $\beta$  expression in the adult cerebellum, where it is restricted to Purkinje cells (Fig. 3). Purkinje cells represent another Dab1-expressing, Reelin-responsive cell type that is not appropriately positioned in Dab1 or Reeler mutant animals.

**Reelin stimulation induces Nck $\beta$  redistribution.** A tyrosine kinase-based signaling cascade has previously been shown to cause a redistribution of Nck $\beta$  (8). Since regulated subcellular compartmentalization is a critical means of regulating protein function, we examined the localization of Nck $\beta$  before and after Reelin stimulation. In the absence of the Reelin signal, the majority of Nck $\beta$  was localized to the cell soma of primary forebrain neurons grown 1 day in vitro (Fig. 4). The majority of neurites expressed very little Nck $\beta$  throughout their length, and the leading edges of the processes were devoid of this adaptor. After 30 min of Reelin stimulation, however, the Nck $\beta$  distribution was changed. Neurites of Reelin-treated cells contained Nck $\beta$ , and the fluorescence was less intense in the cell soma compared to control-treated neurons (Fig. 4).

Nck $\beta$  was observed to be concentrated at the leading edge of processes, at levels comparable to that observed in the cell soma, in approximately 5% of Reelin-treated neurons. The translocation was very rapid, with Nck $\beta$ -enriched regions found at the tip of processes 10 to 15  $\mu$ m away from the soma after 10 min of stimulation with Reelin-enriched medium. Typically, only one process per cell was observed to have a Nck $\beta$ -enriched region, and Dab1 was found to colocalize with Nck $\beta$  in these distal sites in Reelin-treated cultures (Fig. 5).

Nck $\beta$  did not colocalize with Dab1 at the leading edge or growth cones of control-treated cells (Fig. 5). With longer times of stimulation, the percentage of neurons expressing the Nck $\beta$ -enriched regions was reduced (data not shown). In contrast, the process termini of cultured neurons treated with control-conditioned medium showed low levels of Nck $\beta$  (Fig. 5). Reelin stimulation of neurons grown for 7 days in vitro led

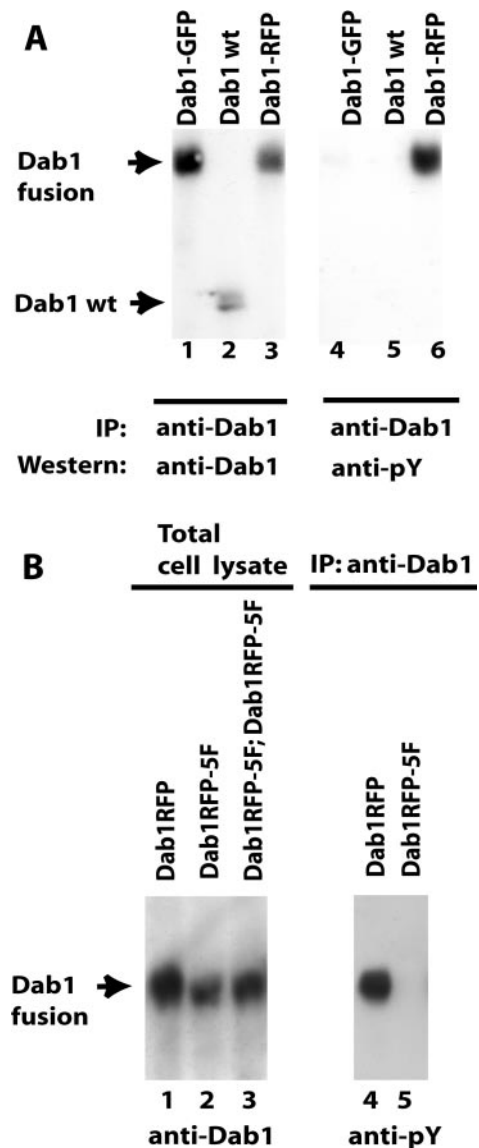


FIG. 6. Mouse Dab1RFP fusion is tyrosine-phosphorylated when expressed in Rat-2 cells and fly eyes. (A) Cell lysates from Rat-2 fibroblasts transfected with Dab1GFP (lanes 1 and 4), Dab1-wt (lanes 2 and 5), or Dab1RFP (lanes 3 and 6) were immunoprecipitated with anti-Dab1 C-terminal antibody. Western blotting with anti-Dab1 antibody (lanes 1 to 3) showed that comparable levels of Dab1 were expressed, but in the antiphosphotyrosine Western blot (lanes 3 to 6), only Dab1RFP (lane 6) was detected. (B) Expression of Dab1RFP and Dab1RFP-5F was detected in total cell lysates of flies with the genotypes *UAS-Dab1RFP/GMR-GAL4* (lane 1), *UAS-Dab1RFP-5F/GMR-GAL4* (lane 2), and *UAS-Dab1RFP-5F;UAS-Dab1RFP-5F/GMR-GAL4* (lane 3) to compare the levels of expression of the wild-type and Dab1-5F mutant flies as adults. Expression of both of these protein products was also observed by Western blot in wandering third-instar larvae and pupae (not shown). Lysates from *UAS-Dab1RFP/GMR-GAL4* (lane 4) and *UAS-Dab1RFP-5F/GMR-GAL4* (lane 5) flies were immunoprecipitated with anti-Dab1 antibody (Chemicon) and Western blotted for antiphosphotyrosine (4G10; Upstate Biotechnology), showing that the Dab1RFP fusion but not the Dab1RFP-5F protein is tyrosine phosphorylated when expressed in the adult fly. The same was observed for wandering third-instar larvae and pupae (not shown).

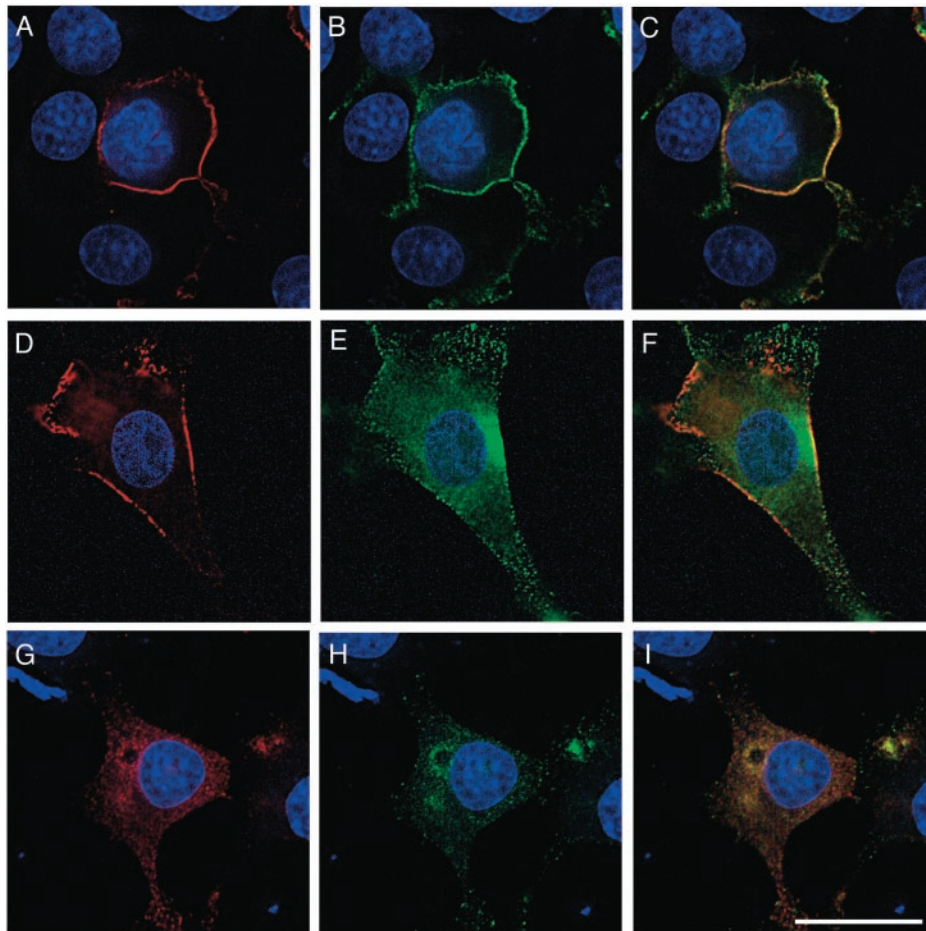


FIG. 7. Nck $\beta$  colocalizes with Dab1 at the cell periphery of Rat-2 fibroblasts in a tyrosine phosphorylation site-dependent manner. (A to C) Dab1RFP (A and C; red) is detected in an intense peripheral ring in the majority of expressing Rat-2 cells, and Nck $\beta$  (B and C; green) is observed to colocalize in this region. (D to F) Dab1RFP-5F (D and F) is expressed in a pattern similar to the wild-type counterpart, however, Nck $\beta$  (E and F) does not colocalize at the cell periphery. (G to I) Native Dab1 (G and I) is predominantly cytoplasmic, and Nck $\beta$  (H and I) is also diffuse throughout the cytoplasm, with no concentration near the plasma membrane. Bar, 20  $\mu$ m.

to the redistribution of Nck $\beta$  away from the cell soma into the processes, but we did not detect the Nck $\beta$ -enriched regions with these older cultures (data not shown).

**Nck $\beta$  overexpressed in the presence of phosphorylated Dab1 alters the actin cytoskeleton.** The Nck family of adaptor proteins plays a conserved role in linking extracellular signals to actin cytoskeletal remodeling (5, 33). To examine if tyrosine-phosphorylated Dab1 could substitute for an external signal and lead to Nck $\beta$ -dependent cytoskeletal rearrangement, we established a cell culture model with Rat-2 fibroblasts. These cells were chosen based on their flat morphology and the relative uniformity of their actin profiles.

To express tyrosine-phosphorylated Dab1 without an activated kinase, we used a Dab1 fusion with red fluorescent protein (Dab1RFP) that we have recently found to be tyrosine phosphorylated in cultured cells (Fig. 6A). Dab1-wt protein, expressed from the RFP vector with a stop codon introduced to prevent fusion to RFP, was not phosphorylated under these culture conditions. Dab1GFP was also not tyrosine-phosphorylated when expressed in Rat-2 cells (Fig. 6A). The tyrosine phosphorylation of Dab1RFP is likely a consequence of mul-

timerization through fusion to the RFP tetramer (V. Strasser, D. Fasching, C. Hauser, H. Mayer, H. H. Bock, T. Hiesberger, J. Herz, E. J. Weeber, J. D. Sweatt, A. Pramatarova, B. Howell, W. J. Schneider, and J. Nimpf, submitted for publication).

Dab1RFP and Dab1RFP-5F were prominently distributed at the cell periphery when expressed in Rat-2 cells, while native Dab1-wt had a more diffuse cytoplasmic distribution (Fig. 7). When Nck $\beta$  was coexpressed with the tyrosine-phosphorylated Dab1RFP, it colocalized at the cell membrane (Fig. 7). In contrast, Nck $\beta$  expressed alone or in combination with native Dab1-wt was found throughout the cytoplasm with no enrichment at the cell membrane. Similarly, expression of Dab1RFP-5F was not capable of recruiting Nck $\beta$  to the cell periphery (Fig. 7). This colocalization at the membrane is suggestive of an *in vivo* association and maybe a mechanism through which Nck $\beta$  is functionally activated.

In the plane of the Rat-2 cell closest to the poly-L-lysine-coated cover glass, we observed a very fine mesh of actin. Overexpression of Nck $\beta$  by three- to fivefold did not detectably alter the actin cytoskeleton (Fig. 8A and B, and data not shown). Expression of Dab1RFP alone resulted in only a mod-

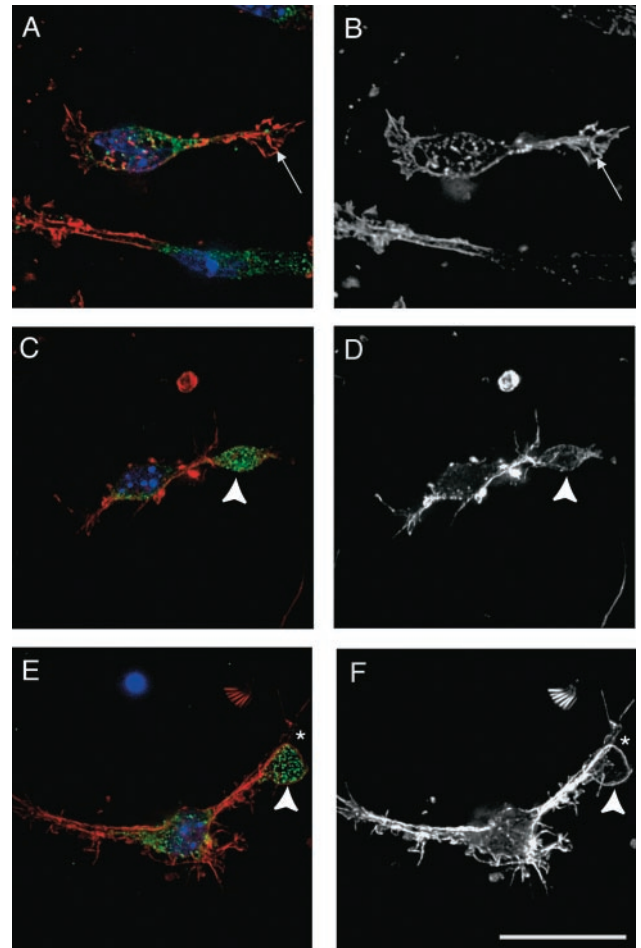
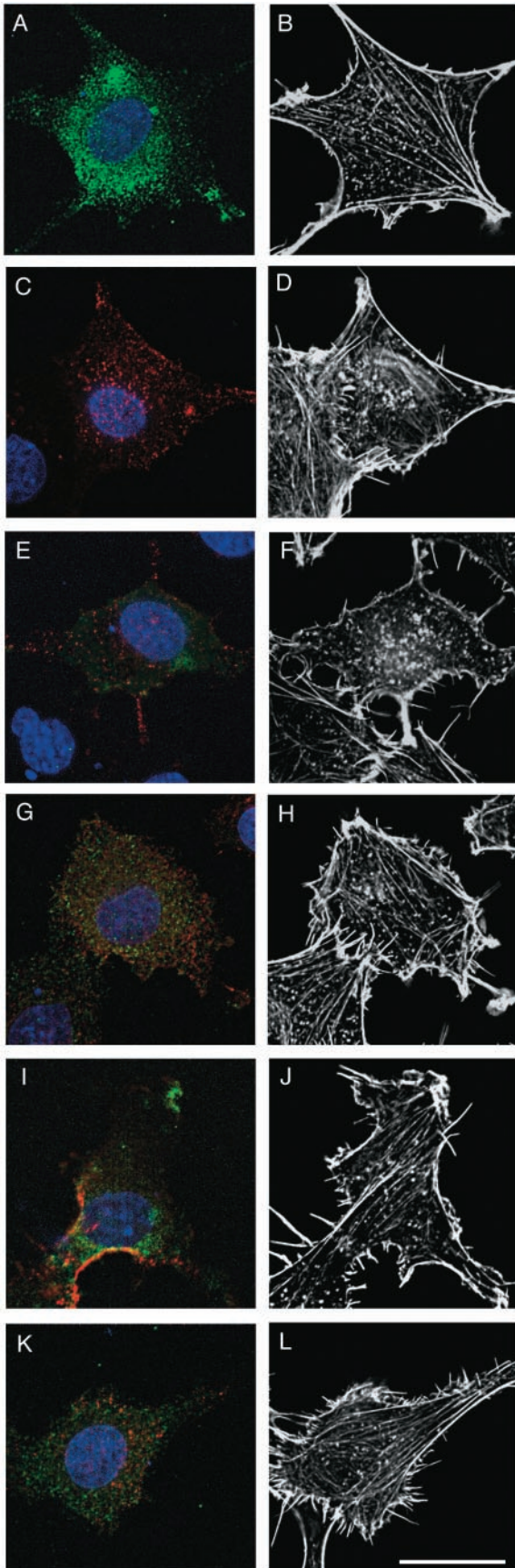


FIG. 9. Nck-enriched regions in distal processes of Reelin-treated neurons have patterns of actin filaments not observed in control-treated neurons. (A and B) The growth cones of neurons at 1 day in vitro demonstrate intense actin filaments (arrow) detected by phalloidin staining (A and B; red and white) and were devoid of Nckβ (green; A). (C to F) Approximately 5% of neurons had Nckβ enrichments in distal processes 10 min after Reelin stimulation (arrowheads). The Nckβ-enriched regions had patterns of actin filaments that varied from actin-poor (C and D) to intense peripheral actin features such as actin rings (star; E and F). Bar, 20 μm.

est loss of regularity of the array of actin (Fig. 8C and D) that may be due to an interaction with low levels of endogenous Nckβ. Overexpression of Nckβ and Dab1RFP, on the other hand, led to a dramatic loss of the actin mesh from the lower

FIG. 8. Coexpression of tyrosine-phosphorylated Dab1RFP and Nckβ in Rat-2 cells leads to the disruption of the actin cytoskeleton. The actin cytoskeleton, detected with fluorescently labeled phalloidin (white; B, D, F, H, J, and L) observed on the lower plane of Rat-2 fibroblasts transfected with HA-Nckβ (green; A and B), or Dab1RFP, a tyrosine-phosphorylated form of Dab1 (red; C and D), shows the typical mesh pattern. Combined expression of HA-Nckβ and Dab1RFP (E and F) leads to disruption of the actin mesh and clumping of actin filaments. Expression of unphosphorylated Dab1-wt with HA-Nckβ (G and H), or Dab1RFP-5F with HA-Nckβ (I and J) did not disrupt the actin cytoskeleton, nor did expression of Dab1RFP with the SH2 domain mutant of Nckβ (K and L). All images show the plane of the cell closest to the cover glass. Bar, 20 μm.



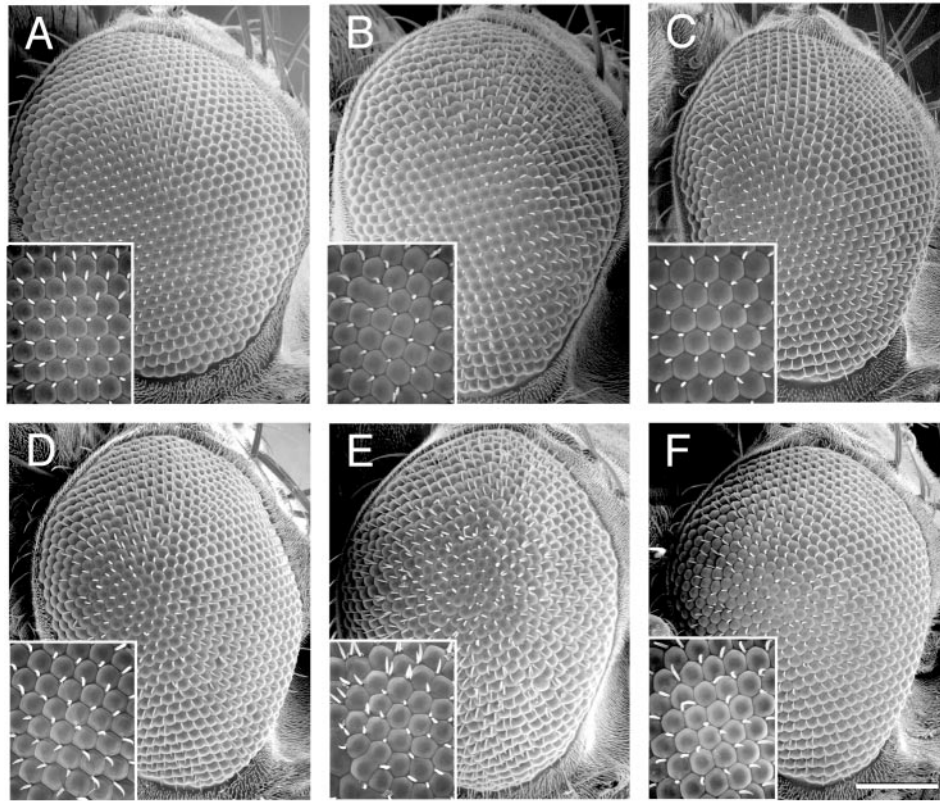


FIG. 10. Overexpression of Dock in the *D. melanogaster* eye enhances a phosphorylation site-dependent Dab1RFP phenotype. Flies with the genotypes *UAS-RFP/GMR-GAL4* (A), *UAS-Dab1RFP/GMR-GAL4* (B), *UAS-Dab1RFP-5F/GMR-GAL4* (C), *UAS-Dock; UAS-RFP/GMR-GAL4* (D), *UAS-Dock; UAS-Dab1RFP/GMR-GAL4* (E), and *UAS-Dock; UAS-Dab1RFP-5F/GMR-GAL4* (F) were examined by scanning electron microscopy. Representative phenotypes are shown from over 10 examples of each genotype that were examined. Expression of the RFP proteins was confirmed by fluorescence microscopy (data not shown). Magnification:  $\times 200$  (scale bar, 100  $\mu\text{m}$ ). Inset magnification:  $\times 1,000$ .

level of the cells and to the appearance of clumps of actin filaments (Fig. 8E and F). In addition, the majority of the cells expressing Nck $\beta$  and Dab1RFP had a rounded or unusual morphology. Expression of Dab1RFP-5F, Dab1-wt, or Dab1GFP in conjunction with Nck $\beta$  overexpression did not disturb the actin scaffolding on the lower surface of the cells (Fig. 8G through J, and data not shown), suggesting that Dab1 phosphorylation is required for the Nck $\beta$ -dependent disruption of the cytoskeleton observed in these cells. Consistent with this finding, overexpression of Dab1RFP in combination with the Nck $\beta$ -R312K SH2 domain mutant did not promote reorganization of the actin cytoskeleton in these cells (Fig. 8K and L).

To determine if Reelin might affect the migratory properties of neurons through effects on the actin cytoskeleton, we investigated the appearance of filamentous actin in cells treated with Reelin or control-conditioned medium. The global appearance of actin was similar between treated and untreated samples. However, we did notice a consistent difference in the actin filaments in Nck $\beta$ -enriched regions of Reelin-treated cells compared to process termini of control-treated cells (Fig. 9). The actin filaments in the Nck $\beta$ -enriched areas were often localized around the periphery or in tight rings (Fig. 9D and F). Actin filaments were scarce in the center of the Nck $\beta$ -enriched regions, and we never observed stress fibers.

The Nck family of adaptors is conserved in organisms such as *Drosophila melanogaster* and *Caenorhabditis elegans*. These proteins are structurally similar throughout the SH3 and SH2 domains and have conserved downstream effectors such as Pak (21, 33). We made use of the conserved nature of these signaling proteins to test for a genetic interaction between mouse Dab1 and *Drosophila* Dock in an eye expression model.

Both Dab1 and Dock were expressed, separately and in combination, in *Drosophila* cells with the upstream activator sequence (UAS)-GAL4 system (4). For this study, we used a glass multimer repeat promoter (*GMR*)-GAL4 line to activate expression of the *UAS-Dab1* or *UAS-Dock* transgenic allele (18). We found that when expressed in the developing *Drosophila*, Dab1RFP is tyrosine phosphorylated (Fig. 6B). The Dab1RFP-5F protein was expressed at slightly lower levels, but no tyrosine phosphorylation was detectable. The expression of Dab1RFP leads to the roughening of the external eye morphology, which is accompanied by loss of linearity of the ommatidial facets and ommatidial fusions (Fig. 10B, insets). In addition, many of the ommatidia have lost the typical hexagonal shape.

The eye morphology, and ommatidial organization or shape are largely unaffected by Dab1RFP-5F expression (Fig. 10C). To account for the lower expression of the *UAS-Dab1RFP-5F*

alleles, we generated flies that carried two copies of the *UAS-Dab1RFP-5F* transgene and one copy of the *GMR-GAL4* transgene. These flies expressed Dab1RFP-5F at levels that were comparable to the Dab1RFP expression levels and did not show defects in external eye morphology (Fig. 6B). The RFP expression did not alter eye morphology from that of the wild type (Fig. 10A). Other controls such as the *UAS-Dab1RFP* and *UAS-Dab1RFP-5F* transgenic lines in the absence of *GMR-GAL4* were indistinguishable from the normal flies (data not shown).

We observed that in flies that coexpressed Dab1RFP and Dock, the severity of the eye roughness was enhanced (Fig. 10E). In these compound eyes, there were many more fusions, and the size of the ommatidia was variable. In contrast, the eyes of flies expressing the Dab1RFP-5F and Dock proteins were not more disorganized than those of flies expressing the Dock or Dab1RFP-5F protein alone, which showed only minor aberrations (Figure 10C, D, and F). This suggests that the Dab1 phosphorylation sites are required for the genetic interaction observed with Dock in this exogenous expression model.

## DISCUSSION

The tyrosine phosphorylation of Dab1 was implicated as a requisite step in Reelin signal transduction. Here we show that a consequence of Dab1 tyrosine phosphorylation is the formation of a complex with the Nck $\beta$  SH2-SH3 domain adaptor molecule. Members of this family of adaptors appear in species from *Drosophila melanogaster* and *Caenorhabditis elegans* to *Homo sapiens* (14, 34). We show that coexpression of tyrosine-phosphorylated mouse Dab1 and the *Drosophila* Nck family member Dock leads to enhancement of the Dab1 expression phenotype in the eye (Fig. 10). This suggests that Nck family members are conserved signaling partners for Disabled family proteins.

The Nck proteins function in tyrosine kinase-based signal transduction cascades and in many instances connect extracellular signals to alterations in the actin cytoskeleton. Of the known SH3 domain binding partners of the Nck proteins, which number over 20, approximately half have direct or indirect roles in the regulation of actin dynamics (33). We provide evidence that one consequence of a Dab1-Nck $\beta$  interaction is alterations in the actin cytoskeleton. Through the analysis of Dab1-signaling partners such as Nck $\beta$ , we hope to gain a better understanding of cell biological changes that are induced by Reelin signaling.

Nck $\beta$  bound tyrosine-phosphorylated Dab1 to a much greater degree than Nck $\alpha$  (Fig. 1). Since the closely related SH2 domains of these two molecules bind different phosphorylation sites on the platelet-derived growth factor receptor, this specificity difference is not unprecedented (7). In addition, the SH2 domain of Nck $\beta$  but not of Nck $\alpha$  was able to bind to the tyrosine-phosphorylated cytoplasmic domain of Ephrin-B1, suggesting that while they are similar, the SH2 domains of Nck $\alpha$  and Nck $\beta$  have different specificities (8). In our in vitro assay, Nck $\beta$  was capable of binding to Dab1 phosphorylated on either Y220 or Y232, which have similar residues C-terminal to the tyrosine, Q-V-P and D-V-P, respectively. This may suggest that valine and pro-

line in the +2 and +3 position relative to the phosphotyrosine may foster the Nck $\beta$  SH2 domain interaction. Both Y220 and Y232 are phosphorylated in embryonic mouse brain (B.Howell, unpublished results); but only Y220 phosphorylation is known to be Reelin inducible (32).

We provide several lines of evidence that support an interaction between Nck $\beta$  and Dab1 in vivo. The protein complex is robust enough to support coimmunoprecipitation from cells overexpressing HA-Nck $\beta$  and tyrosine-phosphorylated Dab1 in the presence of 1% NP-40 (Fig. 2). We observed Nck $\beta$  distribution at the cell periphery of cells expressing tyrosine-phosphorylated Dab1RFP, whereas in cells expressing unphosphorylated versions of Dab1, Nck $\beta$  distribution was exclusively cytoplasmic (Fig. 7). Colocalization between Dab1 and Nck $\beta$  was also apparent at distal sites in processes of neurons treated with Reelin. This was not the case in neurons treated with control-conditioned medium, where Nck $\beta$  protein was predominantly localized in the cell soma (Fig. 4). Taken together, these data suggest that these proteins interact in vivo and that this interaction is dependent upon Dab1 tyrosine phosphorylation.

The redistribution of Dab1 into the processes was rapid. We measured Nck $\beta$  in process tips 10 to 15  $\mu$ m from the cell soma 10 min after Reelin stimulation (Fig. 9). This fast anterograde movement could be mediated by kinesins. The Dab1 PTB domain interacts with two proteins that have been implicated in kinesin-mediated transport. The amyloid precursor protein (APP) binds kinesins directly, and ApoER2 was shown to interact indirectly through association with Jun interacting proteins (30, 49). Dab1 could therefore act to shuttle bound proteins anterograde into distal processes through binding APP or ApoER2.

Nck family proteins are thought to participate in remodeling the actin cytoskeleton upon recruitment to the membrane (5). Since Dab1 is targeted to the membrane through its PTB domain, which binds to cell surface receptors and phospholipids (24, 29, 46), we sought to determine if exogenous expression of tyrosine-phosphorylated Dab1 in the presence of high levels of Nck $\beta$  would alter actin profiles. Overexpressing Nck $\beta$  with Dab1RFP led to disruption of the typical cytoskeletal architecture. Instead, clumps of actin filaments were observed on the lower plane of coexpressing cells (Fig. 8). The disruption of the actin cytoskeleton appears to require the interaction of the two proteins, since either alone had little or no effect. Consistent with this, reorganization of the actin cytoskeleton was not induced when either the Dab1RFP-5F or Nck $\beta$  SH2 domain mutant R312K was substituted for the wild-type proteins. This suggests that tyrosine-phosphorylated Dab1 is capable of substituting for extracellular signals that recruit Nck $\beta$  to effect changes in the actin cytoskeleton.

The demonstration that Nck $\beta$  binds Dab1 and redistributes in Reelin stimulated nascent neurons suggests Reelin may regulate actin dynamics. We did not observe a global difference in actin profiles between fixed neurons from cultures stimulated with Reelin or control conditioned medium. The actin cytoskeleton in the Reelin-induced Nck $\beta$ -enriched regions, however, differs from patterns typically observed in growth cones or process terminals of control cultures (Fig. 9). While the actin filament distribution was variable, a circle of actin filaments was often seen demarcating the Nck $\beta$ -enriched regions.

We consistently observed that the Nck $\beta$ -enriched regions were devoid of actin stress fibers, which are routinely observed at process termini in the control cultures.

Other systems have provided clues to Nck $\beta$  function downstream of extracellular signals. In *D. melanogaster*, the Nck family member Dock transmits signals that regulate the targeting of axonal growth cones. In its absence, the growth cones of the R1 to R6 photoreceptor cells fail to terminate in the lamina and instead migrate into the medulla (14). In mammals it has recently been shown that Nck $\beta$  interacts with the transmembrane Ephrin-B1 ligand, which regulates cell sorting and axonal repulsion (8). In response to stimulation with Eph receptors, expressed on adjacent cells, the transmembrane ligand becomes tyrosine phosphorylated, promoting an interaction with the Nck $\beta$  SH2 domain. This interaction leads to the loss of stress fibers as well as the redistribution of paxillin from the cell periphery into the cytoplasm, suggesting a loss of focal contacts (8).

These cellular changes may be promoted by the numerous Nck $\beta$  SH3 domain-binding proteins. Among them, a number regulate the activity of the Rho family of small GTPases. These include Dock180, an exchange factor for Rac, hnRNPK, which binds to Vav, also a RacGEF, and Pak1, which regulates both Rac and Rho (8, 33, 48). Interestingly it has recently been demonstrated that Reelin stimulation leads to the activation of phosphoinositide 3-kinase (2), which in some signaling scenarios leads to activation of Rac. The kinase CDK5 activator p35 was suggested to regulate neuronal positioning in part by regulating the activity of Rac and the Pak1 kinase (22, 37). The Reelin and CDK5 pathways have synergistic roles in regulating neuronal placement (39). It will therefore be interesting to determine if Reelin acts through Dab1 and Nck $\beta$  to regulate the activity of the Rho family GTPases.

#### ACKNOWLEDGMENTS

We gratefully acknowledge Jon Cooper for support during the initial phase of this project and continuing encouragement, advice, and thoughtful comments on the manuscript. We appreciate the numerous gifts of reagents from Wei Li, Mark Henkemeyer, Chad Cowan, and Laurent Seroude. We value the many discussions on this work from the members of the Neurogenetics Branch. Technical support was provided by Jim Nagle with the NINDS sequencing facility.

This work was supported by NINDS intramural funds, an HHMI physician postdoctoral research fellowship to A.G., and HHMI-NIH research scholarships to S.M. and P.O.

#### REFERENCES

- Arnaud, L., B. A. Ballif, E. Förster, and J. A. Cooper. 2003. Fyn tyrosine kinase is a critical regulator of Disabled-1 during brain development. *Curr. Biol.* **13**:9–17.
- Beffert, U., G. Morfini, H. H. Bock, H. Reyna, S. T. Brady, and J. Herz. 2002. Reelin-mediated signaling locally regulates protein kinase B/Akt and glycogen synthase kinase 3 $\beta$ . *J. Biol. Chem.* **277**:49958–49964.
- Bock, H. H., and J. Herz. 2003. Reelin activates Src family tyrosine kinases in neurons. *Curr. Biol.* **13**:18–26.
- Brand, A. H., and N. Perrimon. 1993. Targeted gene expression as a means of altering cell fates and generating dominant phenotypes. *Development* **118**:401–415.
- Buday, L., L. Wunderlich, and P. Tamas. 2002. The Nck family of adapter proteins: regulators of actin cytoskeleton. *Cell Signal.* **14**:723–731.
- Carlberg, K., and L. R. Rohrschneider. 1997. Characterization of a novel tyrosine-phosphorylated 100-kDa protein that binds to SHP-2 and phosphatidylinositol 3'-kinase in myeloid cells. *J. Biol. Chem.* **272**:15943–15950.
- Chen, M., H. She, A. Kim, D. T. Woodley, and W. Li. 2000. Nckbeta adapter regulates actin polymerization in NIH 3T3 fibroblasts in response to platelet-derived growth factor bb. *Mol. Cell. Biol.* **20**:7867–7880.
- Cowan, C. A., and M. Henkemeyer. 2001. The SH2/SH3 adaptor Grb7 transduces B-ephrin reverse signals. *Nature* **413**:174–179.
- D'Arcangelo, G., R. Homayouni, L. Keshvara, D. S. Rice, M. Sheldon, and T. Curran. 1999. Reelin is a ligand for lipoprotein receptors. *Neuron* **24**:471–479.
- D'Arcangelo, G., G. G. Miao, S. C. Chen, H. D. Soares, J. I. Morgan, and T. Curran. 1995. A protein related to extracellular matrix proteins deleted in the mouse mutant *reeler*. *Nature* **374**:719–723.
- D'Arcangelo, G., G. G. Miao, and T. Curran. 1996. Detection of the *reelin* breakpoint in *reeler* mice. *Brain Res. Mol. Brain Res.* **39**:234–236.
- D'Arcangelo, G., K. Nakajima, T. Miyata, M. Ogawa, K. Mikoshiba, and T. Curran. 1997. Reelin is a secreted glycoprotein recognized by the CR-50 monoclonal antibody. *J. Neurosci.* **17**:23–31.
- Desai, C. J., P. A. Garrity, H. Keshishian, S. L. Zipursky, and K. Zinn. 1999. The Drosophila SH2-SH3 adapter protein Dock is expressed in embryonic axons and facilitates synapse formation by the RP3 motoneuron. *Development* **126**:1527–1535.
- Garrity, P. A., Y. Rao, I. Salecker, J. McGlade, T. Pawson, and S. L. Zipursky. 1996. Drosophila photoreceptor axon guidance and targeting requires the dreadslocks SH2/SH3 adapter protein. *Cell* **85**:639–650.
- Goldowitz, D., R. C. Cushing, E. Laywell, G. D'Arcangelo, M. Sheldon, H. O. Sweet, M. Davison, D. Steindler, and T. Curran. 1997. Cerebellar disorganization characteristic of reeler in scrambler mutant mice despite presence of reelin. *J. Neurosci.* **17**:8767–8777.
- Gupta, A., L. H. Tsai, and A. Wynshaw-Boris. 2002. Life is a journey: a genetic look at neocortical development. *Nat. Rev. Genet.* **3**:342–355.
- Hammond, V., B. Howell, L. Godinho, and S.-S. Tan. 2001. Disabled-1 functions cell autonomously during radial migration and cortical layering of pyramidal neurons. *J. Neurosci.* **21**:8798–8808.
- Hay, B. A., T. Wolff, and G. M. Rubin. 1994. Expression of baculovirus P35 prevents cell death in Drosophila. *Development* **120**:2121–2129.
- Herz, J. 2001. The LDL receptor gene family: (un)expected signal transducers in the brain. *Neuron* **29**:571–581.
- Hiesberger, T., M. Trommsdorff, B. W. Howell, A. Goffinet, M. C. Mumby, J. A. Cooper, and J. Herz. 1999. Direct binding of Reelin to VLDL receptor and ApoE receptor 2 induces tyrosine phosphorylation of disabled-1 and modulates tau phosphorylation. *Neuron* **24**:481–489.
- Hing, H., J. Xiao, N. Harden, L. Lim, and S. L. Zipursky. 1999. Pak functions downstream of Dock to regulate photoreceptor axon guidance in Drosophila. *Cell* **97**:853–863.
- Homayouni, R., and T. Curran. 2000. Cdk5 gets into sticky situations. *Curr. Biol.* **10**:R331–R334.
- Homayouni, R., D. S. Rice, and T. Curran. 2001. Disabled-1 interacts with a novel developmentally regulated protocadherin. *Biochem. Biophys. Res. Commun.* **289**:539–547.
- Homayouni, R., D. S. Rice, M. Sheldon, and T. Curran. 1999. Disabled-1 binds to the cytoplasmic domain of amyloid precursor-like protein 1. *J. Neurosci.* **19**:7507–7515.
- Howell, B. W., F. B. Gertler, and J. A. Cooper. 1997. Mouse disabled (mDab1): a Src binding protein implicated in neuronal development. *EMBO J.* **16**:1165–1175.
- Howell, B. W., R. Hawkes, P. Soriano, and J. A. Cooper. 1997. Neuronal position in the developing brain is regulated by mouse disabled-1. *Nature* **389**:733–737.
- Howell, B. W., T. M. Herrick, and J. A. Cooper. 1999. Reelin-induced tyrosine phosphorylation of disabled 1 during neuronal positioning. *Genes Dev.* **13**:643–648.
- Howell, B. W., T. M. Herrick, J. D. Hildebrand, Y. Zhang, and J. A. Cooper. 2000. Dab1 tyrosine phosphorylation sites relay positional signals during mouse brain development. *Curr. Biol.* **10**:877–885.
- Howell, B. W., L. M. Lanier, R. Frank, F. B. Gertler, and J. A. Cooper. 1999. The disabled 1 phosphotyrosine-binding domain binds to the internalization signals of transmembrane glycoproteins and to phospholipids. *Mol. Cell. Biol.* **19**:5179–5188.
- Kamal, A., G. B. Stokin, Z. Yang, C. H. Xia, and L. S. Goldstein. 2000. Axonal transport of amyloid precursor protein is mediated by direct binding to the kinesin light chain subunit of kinesin-I. *Neuron* **28**:449–459.
- Keegan, K., and J. A. Cooper. 1996. Use of the two hybrid system to detect the association of the protein-tyrosine-phosphatase, SHPTP2, with another SH2-containing protein, Grb7. *Oncogene* **12**:1537–1544.
- Keshvara, L., D. Benhayon, S. Magdaleno, and T. Curran. 2001. Identification of reelin-induced sites of tyrosyl phosphorylation on disabled 1. *J. Biol. Chem.* **276**:16008–16014.
- Li, W., J. Fan, and D. T. Woodley. 2001. Nck/Dock: an adapter between cell surface receptors and the actin cytoskeleton. *Oncogene* **20**:6403–6417.
- Li, W., and H. She. 2000. The SH2 and SH3 adapter Nck: a two-gene family and a linker between tyrosine kinases and multiple signaling networks. *Histol. Histopathol.* **15**:947–955.
- Lioubin, M. N., P. A. Algate, S. Tsai, K. Carlberg, R. Aebersold, and L. R. Rohrschneider. 1996. p150Ship, A signal transduction molecule with inositol polyphosphate-5-phosphatase activity. *Genes Dev.* **10**:1084–1095.
- Maricich, S. M., E. C. Gilmore, and K. Herrup. 2001. The role of tangential migration in the establishment of mammalian cortex. *Neuron* **31**:175–178.
- Nikolic, M., M. M. Chou, W. Lu, B. J. Mayer, and L. H. Tsai. 1998. The

- p35/Cdk5 kinase is a neuron-specific Rac effector that inhibits Pak1 activity. *Nature* **395**:194–198.
38. **Ogawa, M., T. Miyata, K. Nakajima, K. Yagyu, M. Seike, K. Ikenaka, H. Yamamoto, and K. Mikoshiba.** 1995. The *reeler* gene-associated antigen on Cajal-Retzius neurons is a crucial molecule for laminar organization of cortical neurons. *Neuron* **14**:899–912.
  39. **Ohshima, T., M. Ogawa, Veeranna, M. Hirasawa, G. Longenecker, K. Ishiguro, H. C. Pant, R. O. Brady, A. B. Kulkarni, and K. Mikoshiba.** 2001. Synergistic contributions of cyclin-dependant kinase 5/p35 and Reelin/Dab1 to the positioning of cortical neurons in the developing mouse brain. *Proc. Natl. Acad. Sci. USA* **98**:2764–2769.
  40. **Rice, D. S., and T. Curran.** 2001. Role of the reelin signaling pathway in central nervous system development. *Annu. Rev. Neurosci.* **24**:1005–1039.
  41. **Rice, D. S., M. Sheldon, G. D'Arcangelo, K. Nakajima, D. Goldowitz, and T. Curran.** 1998. Disabled-1 acts downstream of *Reelin* in a signaling pathway that controls laminar organization in the mammalian brain. *Development* **125**:3719–3729.
  42. **Ross, M. E., and C. A. Walsh.** 2001. Human brain malformations and their lessons for neuronal migration. *Annu. Rev. Neurosci.* **24**:1041–1070.
  43. **Schneider, C., R. A. Newman, D. R. Sutherland, U. Asser, and M. F. Greaves.** 1982. A one-step purification of membrane proteins with a high efficiency immunomatrix. *J. Biol. Chem.* **257**:10766–10769.
  44. **Sheldon, M., D. S. Rice, G. D'Arcangelo, H. Yoneshima, K. Nakajima, K. Mikoshiba, B. W. Howell, J. A. Cooper, D. Goldowitz, and T. Curran.** 1997. Scrambler and yotari disrupt the disabled gene and produce a reeler-like phenotype in mice. *Nature* **389**:730–733.
  45. **Sweet, H. O., R. T. Bronson, K. R. Johnson, S. A. Cook, and M. T. Davisson.** 1996. *Scrambler*, a new neurological mutation of the mouse with abnormalities of neuronal migration. *Mamm. Genome.* **7**:798–802.
  46. **Trommsdorff, M., J. P. Borg, B. Margolis, and J. Herz.** 1998. Interaction of cytosolic adaptor proteins with neuronal apolipoprotein E receptors and the amyloid precursor protein. *J. Biol. Chem.* **273**:33556–33560.
  47. **Trommsdorff, M., M. Gotthardt, T. Hiesberger, J. Shelton, W. Stockinger, J. Nimpf, R. E. Hammer, J. A. Richardson, and J. Herz.** 1999. Reeler/Disabled-like disruption of neuronal migration in knockout mice lacking the VLDL receptor and ApoE receptor-2. *Cell* **689**–701.
  48. **Tu, Y., D. F. Kucik, and C. Wu.** 2001. Identification and kinetic analysis of the interaction between Nck-2 and DOCK180. *FEBS Lett.* **491**:193–199.
  49. **Verhey, K. J., D. Meyer, R. Deehan, J. Blenis, B. J. Schnapp, T. A. Rapoport, and B. Margolis.** 2001. Cargo of kinesin identified as Jun-interacting protein scaffolding proteins and associated signaling molecules. *J. Cell Biol.* **152**:959–970.
  50. **Vojtek, A. B., and S. M. Hollenberg.** 1995. Ras-Raf interaction: two-hybrid analysis. *Methods Enzymol.* **255**:331–342.
  51. **Ware, M. L., J. W. Fox, J. L. Gonzalez, N. M. Davis, C. Lambert, C. J. Russo, S. C. Chua Jr., A. M. Goffinet, and C. A. Walsh.** 1997. Aberrant splicing of a mouse disabled homolog, mdab1, in the scrambler mouse. *Neuron* **19**:239–249.
  52. **Yip, J. W., Y. P. Yip, K. Nakajima, and C. Capriotti.** 2000. Reelin controls position of autonomic neurons in the spinal cord. *Proc. Natl. Acad. Sci. USA* **97**:8612–8616.